Monolithic High-Tc Superconducting Phase Shifter at 10 GHz

June H. Takemoto-Kobayashi, *Member, IEEE,* Charles M. Jackson, *Member, IEEE,* Emery B. Guillory, Claire Pettiette-Hall, and John F. Burch

***Abstract*—We describe a monolithic high temperature superconductor (HTS) phase shifter integrated into a 10 GHz microstrip line. This is the first demonstration of a nonresonant HTS circuit based on a distributed Josephson inductance approach. We observed phase shifts greater than 150 degrees in resonant structures, and 20 degrees in broadband circuits.**

Introduction

HIGH temperature superconductivity (HTS) can provide high-quality films for passive microwave devices [1], [2], but nonlinear superconducting Josephson elements for active circuits have been difficult to fabricate. Progress in HTS technology enables the fabrication and test of a new broadband HTS phase shifter which employs a high density of superconductive quantum interference devices (SQUIDs). This paper describes the performance of a broadband HTS phase shifter operating at 10 GHz.

Phase shifters are key elements for phased array antennas. A number of uniquely superconducting approaches have been attempted to provide phase control at microwave frequencies [3]. Superconducting phase shift mechanisms include varying the kinetic inductance of thin superconducting films [4], the use of a novel transistor analogy [5], and cascading a series array of Josephson junctions [6].

The distributed Josephson inductance (DJI) approach [7] consists of a superconducting transmission line that is coupled to an array of SQUIDs distributed along its length as shown in Fig. 1. Each SQUID consists of a single HTS microbridge Josephson element shunted by the inductance of the hole in the microstrip line. The Josephson inductance from the SQUIDs provides a variable inductance along the line. By applying flux to the SQUIDs, either through a control current along the transmission line or by an external magnetic field, the inductance distributed along the transmission line can be controlled. The inductance controls the wave velocity, and hence phase delay of the transmission line. The advantages of the DJI phase shifter are that it provides a true time delay phase shift, low loss, and scalability to higher frequencies.

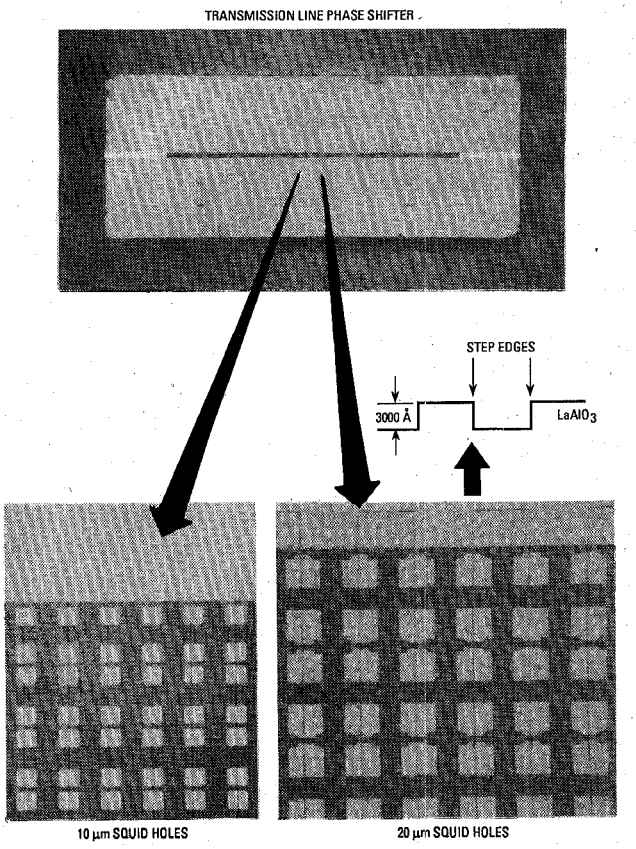

Fig. 1. The nonresonant HTS phase shifter with close-ups of the 10 and 20 μm rf SQUIDs. Dark areas are the YBCO HTS material and the faint rectangular outlines are the steps in the $LaAlO_3$ substrate. Square holes are cut out of the HTS adjacent to narrow 2 μm HTS microbridges which step down over the $LaAlO_3$ step-edges.

We have succeeded in a series of DJI phase shifter demonstrations. Earlier versions of the DJI phase shifter were successfully fabricated and tested in low temperature Nb technology [7]. Later, when HTS SQUIDs became available, a single SQUID was specially selected and coupled to a microstrip resonator [8]. As the maturity of HTS microbridges increased, a total of 40 SQUIDs were monolithically integrated into a single microstrip resonator [9]. The maturity of HTS processing continues to improve, and we have now fabricated and tested a broadband non-resonant HTS phase shifter with greater than 2000 microbridges per wavelength at 10 GHz

Manuscript received March 31, 1992; revised August 3, 1992. This research was funded under the SDIO Materials and Structures Program through ONR contract N00014-91-C-0200.

The authors are with TRW Space and Technology Group, One Space Park, Redondo Beach, CA 90278.

IEEE Log Number 9203698.

monolithically integrated into the active region of the phase shifter.

Fabrication

The new HTS phase shifter requires fabrication of a large array of step-edge HTS SQUIDs [10]. We pattern HTS microbridges over sharp steps etched in the 20-mil thick $LaAlO_3$ substrate. A steep 0.3 μm step is ion-milled into the substrate, and an HTS film (0.2 μm) is deposited over the entire area. The film is then patterned and ion-milled to produce a 2-μm wide microbridge over the step-edge, resulting in an high quality weak link Josephson element.

Fig. 1 shows a photo of the fabricated HTS SQUIDs on the microstrip phase shifters. In the detailed blow up of the active region, the 2-μm step-edge microbridge and the pair of inductive square holes (10 or 20 μm) make up a single rf SQUID. These SQUIDs are duplicated in parallel as a column across the width of the microstrip. These columns of SQUIDs are in turn laid out in series along the length of the resonator or transmission line.

Design and Theory of Operation

The most important properties of the DJI are the response to a control field and the magnitude of the phase shift. This section finds the current per flux quantum I_Φ and the change in inductance normalized to the total inductance per unit length $\Delta L/L$ (which is related to the phase shift). The HTS DJI uses a planar geometry with square holes (of side a) spaced a distance d apart, filling the microstrip line (of width w) over a ground plane a distance h below (Fig. 2). The SQUIDs provide a variable inductance which couples to the transmission line, as shown in Fig. 3.

The change in inductance for a single pair of loops (with a single junction) is determined in two limits. The first limit, a low coupling limit, uses Ampere's law to find the magnetic field and mutual inductance, and the other uses a high coupling limit where the mutual inductance is taken as the loop inductance. Both limits assume that the current is uniform over the microstrip line; a limit that is most valid for wide lines. The current per flux quantum Φ_o can be measured to determine which model is the better estimate. For the low coupling limit,

$$I_\Phi = \frac{2\pi\, dW\, \Phi_o}{3\mu_o a^3} \tag{1}$$

and for the high coupling limit

$$I_\Phi = \frac{4W\Phi_o}{15\mu_o a_2}. \tag{2}$$

We define the following parameters to calculate the total change in inductance:
The coupling constant k,

$$k^2 = \frac{M^2}{L_{\rm sq}L_{\rm ms}}; \tag{3}$$

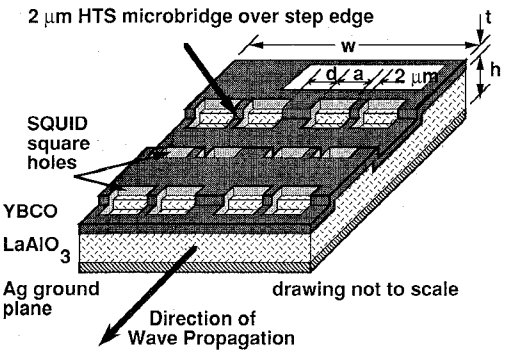

Fig. 2. Perspective drawing of SQUID geometry. Drawing is not to scale. HTS (YBCO) of thickness t (0.3 μm) is deposited on top of a 20-mil (height h) $LaAlO_3$ substrate with 0.6 μm of Ag ground plane. SQUID holes are squares of side a with spacing d apart on a microstrip of width w. Hole pairs are joined by a 2 μm HTS microbridge weak link that steps over a 0.3 μm $LaAlO_3$ step.

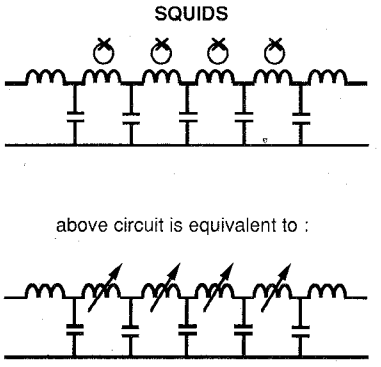

Fig. 3. The equivalent circuit model of a distributed Josephson inductance phase shifter is a network of SQUID inductances coupled to the distributed microstrip inductances and capacitances.

SQUID loop inductance $L_{\rm sq}$,

$$L_{\rm sq} = 1.25\mu_o a; \tag{4}$$

the microstrip inductance $L_{\rm ms}$ (for a length a),

$$L_{\rm ms} = \frac{\mu_o h a}{W}; \tag{5}$$

and the non-hysteretic SQUID criterion for β,

$$\beta = \frac{2\pi L_{\rm sq} I_c}{\Phi_o} < 1. \tag{6}$$

To find the total changes in inductance we combine (1)–(6) with the following equation [7], [11]

$$\frac{\Delta L_{\rm one}}{L_{\rm one}} = k^2\beta. \tag{7}$$

Combining these terms, we obtain a total change in inductance value L_T in the Ampere's Law limit:

$$\frac{\Delta L_T}{L_T} = \frac{6a^4\beta}{5\pi^2 d^2 h(a+d)} \tag{8}$$

and in high coupling limit:

$$\frac{\Delta L_T}{L_T} = \frac{15a^2\beta}{2H(a+d)}. \tag{9}$$

The high coupling limit is about 60 times larger than the Ampere's loop limit. Note that these two expressions do not depend on the width explicitly, but they do depend on the loop size a, spacing d, and substrate height h. In the limit of $a = d$ the change in inductance is proportional to a/h for both the Ampere's loop and high coupling limit calculation. For maximum phase shift, the hole size a should be as large as possible, and h should be as small as possible.

The microbridge critical current Ic is typically between 100 μA (at 4 K) and 30 μA (at 65 K) for 2-μm HTS step-edge microbridges. The condition $\beta = 1$ produces the maximum change in inductance and sets the size of the loops.

The experimental results, provided in the Table I, show that the high coupling limit provides the best estimate on the performance of the devices.

The normalized change in inductance exhibits a periodic response. For the case of a SQUID coupled to a tank circuit [11] or a transmission line [8] this has been shown to be given by

$$\frac{\Delta L}{L_T} = \frac{k^2}{1 + 1/\beta_e \cos(2\pi\phi_e)} \cong k^2\beta_e \cos(2\pi\phi_e). \quad (10)$$

In the limit of small β, the normalized inductance follows a cosine response, but as β increases, the curve shows a more triangular shape.

The actual current per flux quantum data was fitted to a sine curve to determine the periodicity of the $I\phi$ values as shown in Fig. 4(a) and (b). For the 20-μm SQUID nonresonant phase shifter the $I\phi$ was 0.39 mA which is 44 percent of the predicted high coupling limit value. For the 10-μm holes the high coupling limit is even closer; 10 mA compared with 1.1 mA.

The introduction of a dense array of small holes into the microstrip line has a small impact on the microstrip impedance. The additional inductance contributed by the holes in the microstrip can be estimated from the case of a round hole in a stripline geometry [12], [13]. The admittance of the holes in a stripline configuration can be shown to be

$$B_h = \frac{3\lambda hw}{4\pi a^3} = \frac{Z_o}{\omega L} \quad (11)$$

where the wavelength over the hole size λ/a is the important parameter. For small 10 and 20-μm holes, the wavelength is much larger than the hole size, and the additional inductance is small. Solving for the additional inductance, we obtain

$$L = \frac{\mu_o a^3}{6w^2} \quad (12)$$

When compared to the microstrip inductance (5), the additional inductance per unit length is small and easily compensated for, even with a high density of holes.

TABLE I
SUMMARY OF CALCULATED AND MEASURED PARAMETERS OF PHASE SHIFTERS IN A BROADBAND CIRCUIT AT 10 GHz

SQUID size / Coupling Limit	10-μm Hole		20-μm Hole	
	Low	High	Low	High
Lsq	16 pH		32 pH	
β (Ic = 100 μA)	5		10	
$I\phi$ (Theory)	4.3 mA	1.1 mA	0.54 mA	0.27 mA
$I\phi$ (Exp)	1.0 mA		0.39 mA	
$\Delta v_p/v_p$	0.0006	0.037	0.0064	0.098
$\Delta\theta$ (Theory)	0.11°	6.6°	1.15°	17.6°
$\Delta\theta$ (Exp)	8°		20°	

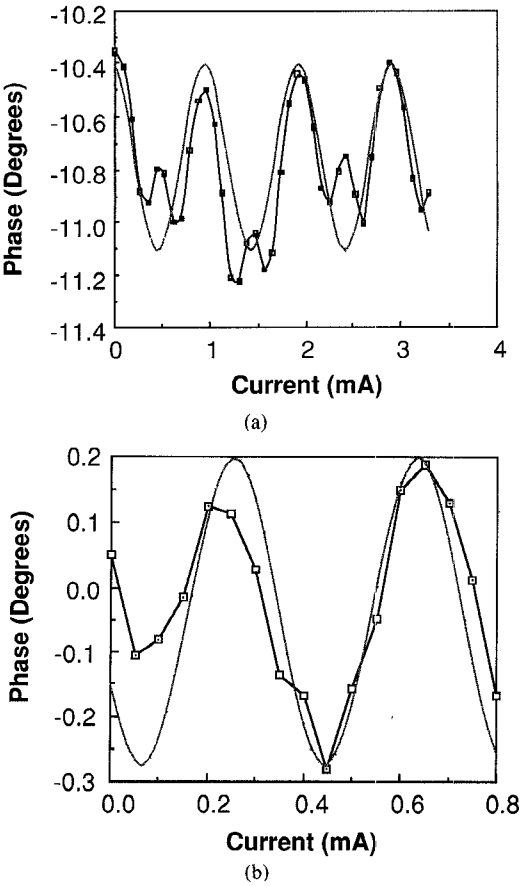

Fig. 4. Phase shift versus control current for 10 and 20-μm circuits. The sine curve is shown for comparison to determine the periodicity (a) 1.0 mA for the 10-μm circuit, and (b) 0.39 mA for the 20-μm.

MEASUREMENTS AND RESULTS

We observed significant phase shifts in both resonant and nonresonant phase shifter at X-band. The resonant circuit consists of hundreds of SQUIDs integrated into the resonant section of a microstrip resonator, whereas the nonresonant version are SQUIDs integrated onto a broadband microstrip transmission line. Most of the results presented here have step-edge junction topology shown in

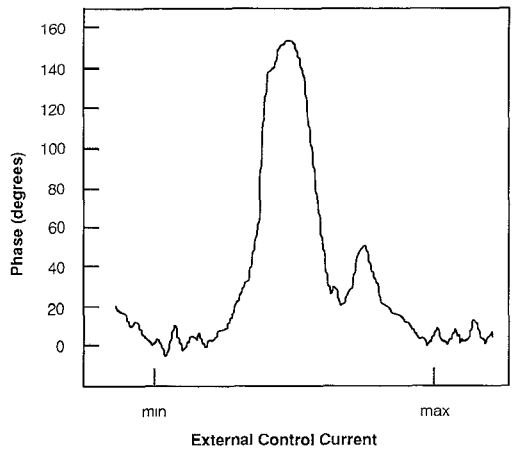

Fig. 5. Phase as a function of external field for resonant phase shifter at 10 GHz at 4 K and −40 dBm input power.

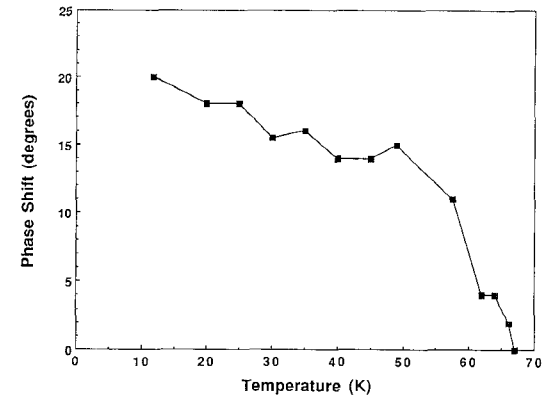

Fig. 7. Temperature dependence of non-resonant 20-μm hole SQUID phase shifter was measured using external field control through transmission line at −30 dBm input power and 9.4 GHz. Phase shift is maintained near 15 degrees from 4.2 K to 50 K. Detectable phase shifts were measured up to 67 K.

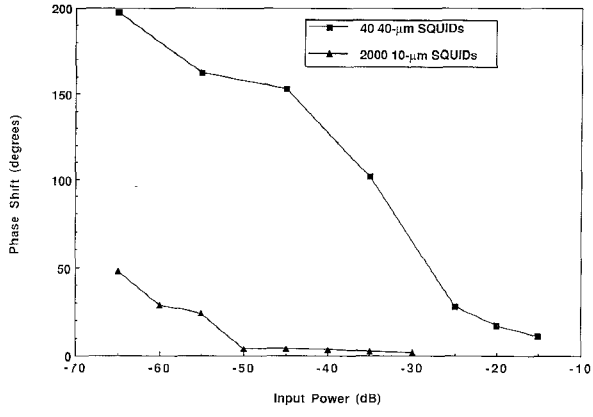

Fig. 6. Plot of peak to peak phase shift versus input power for a resonator with 2000 10-μm hole SQUIDs shows significant improvement in power and phase shift of this work on over a previously reported HTS phase shifter with 40 40-μm hole SQUIDs [6].

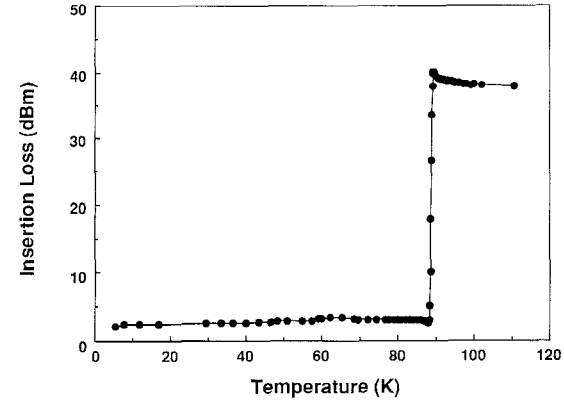

Fig. 8. Insertion loss of a nonresonant phase shifter with 20-μm SQUIDs. Input power of −20 dBm was applied to the circuit.

Figs. 1 and 2. However, phase shifts measured on a nonresonant circuit with more advanced step-edge geometry will also be described.

A resonant structure exhibits an enhanced phase shift as shown by Fig. 5, because the phase changes 190 degrees as the frequency sweeps through the resonance. Measurable phase shifts were detected up to 65 K. Input power was typically set to −40 dBm.

Fig. 6 shows the power dependence of the resonating phase shifter for the new high SQUID density phase shifter as compared to the results reported previously [9]. The newer devices have improved their power handling from −50 dBm to over −10 dBm, while the phase shift has increased from 50 degrees to over 190 degrees. Notice that a phase shift over 180 degrees was achieved due the change in phase velocity caused by kinetic inductance effects of the superconducting microstrip.

Phase change was measured with a modulated magnetic field using either current through external coil or a direct current passed down the transmission line for the straight transmission line phase shifters. When the external coil provided the varying magnetic field, the transmission line circuit shifted phase by 13 degrees at −30 dBm input power. Fig. 7 plots the temperature dependence of the phase shift using this method for a straight through circuit. The insertion loss is shown on Fig. 8 as a function of temperature at −20 dB power.

When direct current is passed down the transmission line shown in Figs. 1 and 2, the circuits yield a phase shift of 20 degrees as shown in Fig. 9. The current per flux quantum of the phase shift using internal control current is 240 μA at 10 K to 14 μA at 67 K. Phase begins shifting significantly near the critical current of HTS circuit which is typically around 100–300 μA. As shown in Fig. 1, the circuit layout we are using has a step-edge all the way across the microstrip, so an alternate circuit model is a series of parallel array of junctions. The series junctions mask the coupling of the control current and limit the maximum current to a value below $I\phi$. This dependence on Ic is similar to that observed by G. Chen for a series array of Josephson junctions [6].

We have compensated this series array effect in a new mask for studying the effect of changing the step-edge area and also by improving the HTS deposition process to prevent weak links from forming outside of the SQUIDs. The newer version uses small step-edge boxes that attempt to

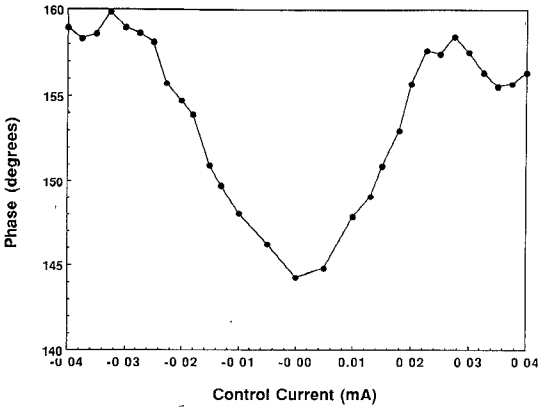

Fig. 9. This plot shows phase shift versus control current where direct current was passed along the straight through transmission line containing the 20-μm hole SQUIDs. Phase was measured at a temperature of 44 K and an input power of -40 dBm.

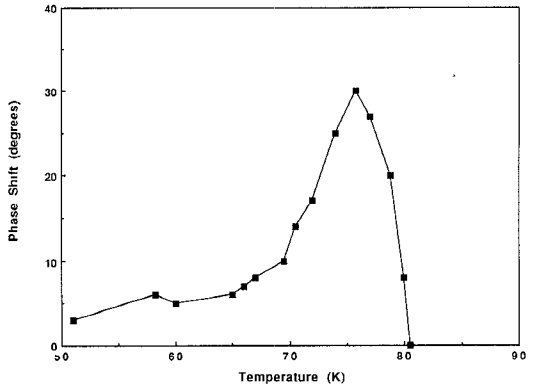

Fig. 10. Temperature dependence of phase for a nonresonant 20-μm SQUID phase shifter with small step-edge areas that do not cross the microstrip area between the SQUIDs. The phase shifts better at higher temperatures and is at its maximum near 77 K where the SQUID beta approaches unity.

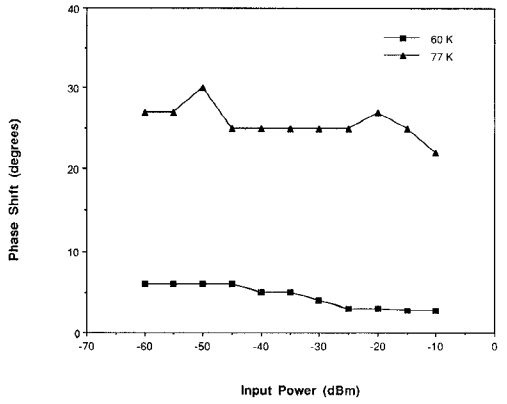

Fig. 11. Power dependence of the same nonresonant 20-μm SQUID phase shifter at 60 K and 77 K.

step only one microbridge at a time. Therefore, higher currents pass down the unstepped regions between the SQUID hole pairs. Fig. 10 shows the phase versus temperature of this alternate type of 20-μm SQUID nonresonant phase shifter. The device does not begin shifting phase significantly until the temperature is above 45 to 50 K where the β is much greater than 1. The phase shift is at its maximum of 30 degrees near 77 K where the β of the SQUIDs approach unity. Fig. 11 shows the power dependence of the same phase shifter at 60 and 77 K. The nonresonant circuit with this alternate version of step-edge junctions maintains its phase shifter at higher input powers and temperatures.

Conclusion

We have presented data on an HTS monolithic phase shifter using over two thousand integrated SQUID devices per wavelength. Phase shifts of 20 degrees were observed in transmission line circuits, and phase shifts of greater than 190 degrees were observed in the resonant circuits. The high coupling limit is the best model for the circuit. This high temperature superconducting phase shifter is suitable for integration into phased array antenna systems for communications applications.

Acknowledgment

The authors would like to thank Kevin W. Kobayashi for his technical advice on microwave propagation, Andrew D. Smith for his comments and suggestions, Dale J. Durand for his technical advice in the theory of SQUIDs, Aron F. Kain for the circuit layout, Chuong Dang for sawing and ribbon bonding of chips, and Alfred Lee for discussions about the deposition process.

References

[1] J. H. Takemoto, C. M. Jackson, R. Hu, J. F. Burch, K. P. Daly, and R. W. Simon, "Microstrip resonators and filters using high-Tc superconducting thin films on $LaAlO_3$," *IEEE Trans. Magn.*, vol. 27, pp. 2549–2552, Mar. 1991.

[2] J. H. Takemoto, C. M. Jackson, H. M. Manasevit, D. C. St. John, J. F. Burch, K. P. Daly, and R. W. Simon, "Microstrip resonators using two-sided metalorganic chemical vapor deposited Er-Ba-Cu-O thin films," *Applied Physics Lett.*, vol. 58, no. 10, pp. 1109–1111, Mar. 11, 1991.

[3] R. C. Hansen, "Antenna applications of superconductivity," *IEEE Trans. Microwave Theory Tech.*, vol. 39, no. 9, pp. 1508–1512, Sept. 1991.

[4] J. M. Pond, J. H. Claassen, W. L. Carter, "Measurements and modeling of kinetic inductance microstrip delay lines," *IEEE Trans. Microwave Theory Tech.*, vol. MTT-35, no. 12, pp. 1256–1262, Dec. 1987.

[5] J. Martens, V. M. Hietala, T. E. Zipperian, D. S. Ginley, C. P. Tigges, and J. M. Phillips, "*S*-parameter measurements and microwave applications of a superconducting flux flow transistor," *IEEE Trans. Microwave Theory Tech.*, vol. 39, no. 12, pp. 2018–2025, Dec. 1991.

[6] G. Chen, "Shock-wave generation and pulse sharpening on a series array Josephson function transmission line," *IEEE Trans. Applied Superconductivity*, vol. 1, no. 3, pp. 140–144, Sept. 1991.

[7] D. J. Durand, J. Carpenter, E. Ladizinsky, L. Lee, C. Jackson, A. H. Silver, and A. D. Smith, "The distributed Josephson inductance phase shifter," *IEEE Trans. Applied Superconductivity*, vol. 2, no. 1, pp. 33–38, Mar. 1992.

[8] C. M. Jackson, and D. J. Durand, "10 GHz high temperature superconductor phase shifter," in *1991 IEEE MTT-S Microwave Symp. Dig.*, June 1991.

[9] J. H. Takemoto-Kobayashi, C. M. Jackson, C. Pettiette-Hall, J. F. Burch, "High-Tc superconductor monolithic phase shifter," *IEEE Trans. Applied Superconductivity*, vol. 2, no. 1, pp. 39–44, Mar. 1992.

[10] K. P. Daly, W. D. Dozier, J. F. Burch, S. B. Coons, R. Hu, C. E.

Platt, and R. W. Simon, "Substrate step-edge $YBa_2Cu_3O_7$ rf SQUIDs," *Applied Physics Lett.*, vol. 58, no. 4, pp. 543–545, Feb. 4, 1991.
[11] A. Barone and G. Paterno, *Physics and Applications of the Josephson Effect*. New York: Wiley-Interscience, 1982, pp. 384.
[12] H. M. Altschuler and A. A. Oliner, "Discontinuities in the Center Conductor of Symmetric Strip Transmission Lines," *IRE Trans. Microwave Theory Tech.*, vol. MTT-8, pp. 328–339, May 1960.
[13] K. C. Grupta, R. Garg, R. Chadha, *Computer-Aided Design of Microwave Circuits*. Norwood, MA: Artech House, 1981, pp. 179–201.

June H. Takemoto-Kobayashi (S'82–M'91) received the B.S.E.E. and M.S.E.E. degrees from the University of California, Los Angeles, in 1986 and 1988, respectively.

She has worked at Rockwell International for two summers in 1982 and 1983, analyzing the structural stress on space shuttle vehicles. In 1984 she joined the Radar Design Department of Missile Systems Group at Hughes Aircraft, simulating the performance of AMRAAM missiles' target acquisition and tracking capabilities in various scenarios. She joined TRW in 1986 and worked in the Gallium Arsenide Integrated Circuits Department for two years doing development and research on GaAs metal semiconductor field effect transistor process and device design. In 1988 she transferred to the Superconductive Electronics Research Group and is presently designing and testing microwave devices such as resonators, filters, and phase shifters using high temperature superconductor films on $LaAlO_3$ substrates. She has published several papers on superconducting microwave devices.

Charles M. Jackson (M'83) received the Ph.D. degree in solid-state physics from the University of California at Los Angeles in 1983.

He spent two years with Hughes Aircraft Co., Torrance, CA, where he developed millimeter wave technology and cryogenic mixers. He then joined TRW, where he developed millimeter wave mixers, quasi-optical technology, and ferrite devices. He is currently developing high temperature superconducting technology for microwave applications in TRW's Superconducting Electronics Department, Advanced Technology Division. He is the author of papers on quasi-optical mixers and superconducting microwave devices.

Dr. Jackson is a member of the Microwave Techniques and Technology Society, and is active in his local chapter, having served as Chapter Chairman and Treasurer. He is also a member of the American Physical Society.

Emery B. Guillory received the B.S. degree in 1989 from California University Northridge in the field of electrical engineering and is currently working on a M.S. degree at Northridge with emphasis in applied electromagnetics, microwave and solid state devices.

He is currently employed with EEsof Inc., Westlake Village where his duties consist of support of nonlinear circuit simulation and electromagnetic simulation of planar devices. His interests include time domain electromagnetic wave modeling of biological media, millimeter wave circuit design, nonlinear optics, and developing effective strategies in marketing new technologies.

Claire Pettiette-Hall received the B.S. degree in chemistry from Yale University, New Haven, CT, in 1983 and the Ph.D. degree in physical chemistry from Rice University, Houston, TX, in 1988. She was two year Post-Doctoral Appointee at the University of California, Irvine.

She joined the Superconductive Electronics Research Group at TRW in 1990, where her research is currently focused on the use of laser ablation for epitaxial film growth of materials associated with high temperature superconducting electronic devices.

John F. Burch has been with TRW for 19 years and is currently a Member of Technical Staff with the Superconductive Electronic Research Department of TRW's Space and Technology Group. He is involved in developing lithography for use in high temperature superconductor processing as well as thin film deposition and vacuum system design. He also maintains the substrate step edge etch process. He has previously been involved with development work on the NASA 20/30-GHz GaAs FET power amplifier and a niobium-based Josephson four channel radiometer.